

# Challenges in locating the QCD critical point via constant entropy density contours

Michał Marczenko,<sup>1,\*</sup> Michał Szymański,<sup>2,†</sup> and Győző Kovács<sup>2,3,‡</sup>

<sup>1</sup>*Incubator of Scientific Excellence - Centre for Simulations of Superdense Fluids,  
University of Wrocław, plac Maksa Born 9, PL-50204 Wrocław, Poland*

<sup>2</sup>*Institute of Theoretical Physics, University of Wrocław,  
plac Maksa Born 9, PL-50204 Wrocław, Poland*

<sup>3</sup>*Institute for Particle and Nuclear Physics, HUN-REN Wigner Research Centre for Physics,  
1121 Budapest, Konkoly-Thege Miklós út 29-33, Hungary*

(Dated: April 8, 2025)

A new method was proposed recently to investigate the location of the putative critical point of strongly interacting matter, governed by quantum chromodynamics. By approximating contours of constant entropy density at finite baryon chemical potential, the conditions for the existence of a critical point are solved. In this work, we analyze this method in the hadron resonance gas and Nambu–Jona-Lasinio models. We demonstrate that the prediction of the critical point in the HRG model is solely due to mesonic and baryonic degrees of freedom, and thus is not necessarily a signal of a critical point. We argue that such an expansion leads to a physically meaningful prediction only when applied near the critical point.

## I. INTRODUCTION

One of the key tasks addressed in the context of high-energy physics is the determination of the phase diagram of Quantum Chromodynamics (QCD) at finite temperature and baryon chemical potential. At low baryon chemical potential and high temperature, the transition from hadronic to quark-gluon plasma phase is smooth and is connected with the restoration of chiral symmetry [1–5]. On the other hand, based on the effective model calculations, one expects a first-order phase transition at large baryon chemical potential and low temperature [6–9]. This would imply the presence of a putative critical point (CP) on the QCD phase diagram. Throughout recent years experimental attempts have been made to locate it on the QCD phase diagram. Despite enormous experimental effort within the beam energy scan (BES) programs at the Relativistic Heavy Ion Collider (RHIC) at BNL [10] and the Super Proton Synchrotron (SPS) at CERN [11], this pressing issue remains unresolved (for a recent review see [12]).

A new method for locating the QCD CP was recently proposed [13]. It is based on the fact that thermodynamic quantities, such as entropy, are multi-valued between the spinodals of the first-order phase transition. This leads to the crossing of lines of different constant entropies in the first-order region. Thus, constant-entropy contours at finite temperature and baryon chemical potential can be used to locate the onset of a first-order phase transition and, therefore, the location of a critical endpoint. In [13], the constant-entropy contours were approximated via the Taylor series at vanishing baryon chemical potential to predict the existence of a CP. The constant-

entropy-contour scheme was recently used in LQCD simulations to exclude the location of CP at  $\mu_B < 450$  MeV at  $2\sigma$  confidence level [14].

In this work, we apply the constant-entropy expansion scheme to the hadron resonance gas (HRG) and Nambu–Jona-Lasinio (NJL) models to test its predictive power for the CP. Both models are extensively studied at finite temperature and baryon chemical potential. The HRG model has been successful in describing LQCD data on the EoS and fluctuations of conserved charges at vanishing baryon chemical potential [15, 16] as well as the hadron yields from heavy-ion collisions [17]. The NJL model describes the effective interactions of quarks preserving the chiral symmetry of the massless QCD Lagrangian. We demonstrate that the constant-entropy expansion scheme leads to the unphysical prediction of the existence of CP in the HRG model, which does not implement any criticality. In addition, we directly compare the results obtained in the full NJL model (which may or may not predict a CP, depending on its details), with the prediction obtained through the constant-entropy expansion scheme.

This paper is organized as follows. In Sec. II, we introduce the constant-entropy expansion scheme. In the following two sections, we discuss the results obtained within the HRG and NJL models. The last section concludes our findings.

## II. TAYLOR EXPANSION OF THE CONSTANT-ENTROPY CONTOURS

The method proposed in [13] considers the contours of constant entropy density,  $s$ , at finite  $T$  and  $\mu_B$ , i.e.,

$$s(T_s(T, \mu_B), \mu_B) = s(T, \mu_B = 0) \quad (1)$$

The temperature contour  $T_s(T, \mu_B)$  is chosen such that the entropy is fixed at arbitrary  $\mu_B$ . The profile

\* michal.marczenko@uwr.edu.pl

† michal.szymanski@uwr.edu.pl

‡ gyozo.kovacs@uwr.edu.pl

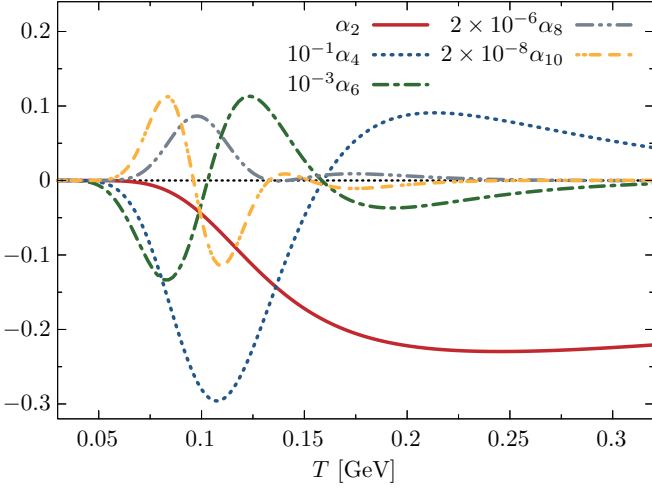


FIG. 1. Temperature dependence of the expansion coefficients,  $\alpha_2$ ,  $\alpha_4$ ,  $\alpha_6$ ,  $\alpha_8$ , and  $\alpha_{10}$ . Note that the coefficients are rescaled for better presentation.

$T_s(T, \mu_B)$  can be expanded into Taylor series around  $\mu_B = 0$ ,

$$T_s(T, \mu_B) = T + \sum_{k=1}^{\infty} \frac{\alpha_k}{k!} \mu_B^k, \quad (2)$$

where

$$\alpha_k = \left. \frac{d^k T}{d\mu_B^k} \right|_s. \quad (3)$$

It is understood that the coefficients  $\alpha_k$  depend on the temperature  $T$ , i.e.,  $\alpha_k = \alpha_k(T)$ . Since odd coefficients  $\alpha_{2k+1}$  vanish at  $\mu_B = 0$ , the lowest-order non-vanishing coefficient is  $\alpha_2$ , which reads

$$\alpha_2 = - \left. \frac{\partial^2 s}{\partial \mu_B^2} \right|_T \bigg/ \left. \frac{\partial s}{\partial T} \right|_{\mu_B}, \quad (4)$$

where

$$s = \left. \frac{\partial P}{\partial T} \right|_{\mu_B} \quad (5)$$

is the entropy density. The higher-order coefficients are more complicated functions of entropy and its derivatives with respect to the temperature and/or baryon chemical potential. In general, the following recursive relation holds for  $k > 0$ :

$$\alpha_{k+1} = \left. \frac{d^{k+1} T}{d\mu_B^{k+1}} \right|_s = \left. \frac{d\alpha_k}{d\mu_B} \right|_s = \left. \frac{\partial \alpha_k}{\partial \mu_B} \right|_T + \alpha_1 \left. \frac{\partial \alpha_k}{\partial T} \right|_{\mu_B}, \quad (6)$$

from which  $\alpha_k$  for  $k > 2$  can be systematically derived starting from Eq. (4).

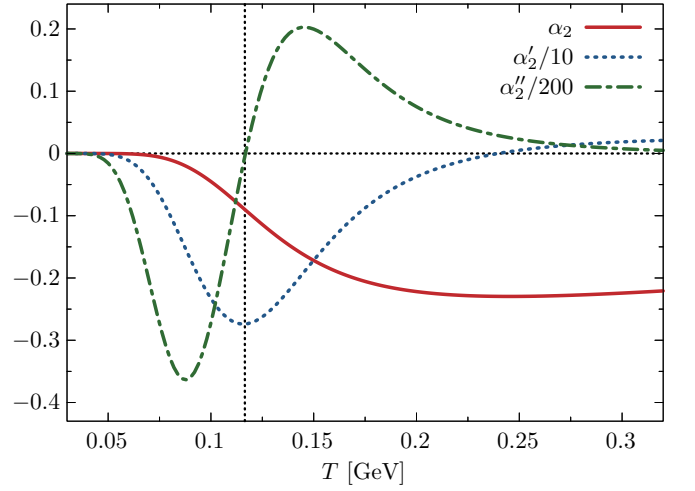


FIG. 2. The second order expansion coefficient  $\alpha_2$ , its first ( $\alpha'_2$ ) and second ( $\alpha''_2$ ) derivatives w.r.t temperature. The vertical, dotted line marks the temperature at which the second derivative vanishes, i.e.,  $\alpha''_2 = 0$ . The first and second derivatives are rescaled for better presentation.

In principle, the critical point can be located through the equations

$$\left. \frac{\partial T_s}{\partial s} \right|_{\mu_B} = 0, \quad \left. \frac{\partial^2 T_s}{\partial s^2} \right|_{\mu_B} = 0. \quad (7)$$

Truncating the Taylor series at the lowest-order ( $k = 2$ ), the criteria can be written with the temperature derivatives of  $\alpha_2$ ,

$$2 + \frac{d\alpha_2}{dT} \mu_B^2 = 0, \quad \frac{d^2 \alpha_2}{dT^2} = 0. \quad (8)$$

Solving these equations yields a prediction for the location of the CP in terms of the critical temperature  $T_c$  and baryon chemical potential  $\mu_{B,c}$  [13],

$$\mu_{B,c} = \sqrt{-\frac{2}{\alpha'_2(T_{0,c})}} \\ T_c = T_{0,c} + \alpha_2(T_{0,c}) \frac{\mu_{B,c}^2}{2}, \quad (9)$$

where  $T_{0,c}$  is obtained from the second of Eqs. (8). We note that the criteria in Eq. (8) predict the existence of the CP at the real baryon chemical potential for  $d\alpha_2/dT < 0$ , that is, when  $\alpha_2$  features an inflection point with a negative slope.

### III. HADRON RESONANCE GAS MODEL

In the phenomenological description of hadronic matter, one needs to identify the relevant degrees of freedom and the interactions among them. In the confined

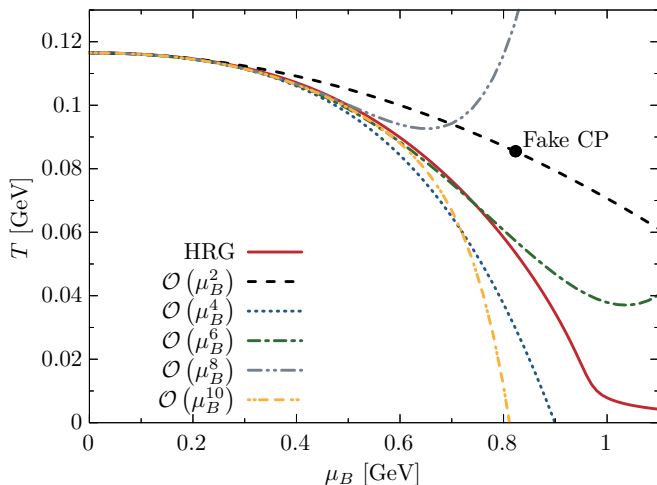


FIG. 3. Constant-entropy contour obtained in the HRG model starting at  $\mu_B = 0$  and  $T$  such that  $\alpha_2'' = 0$ , which leads to the prediction of a fake CP, shown as a black circle on the contour obtained with the  $\mathcal{O}(\mu_B^2)$  truncation of the Taylor series defined in Eq. (2) (see text for details). Shown are also contours obtained with higher-order truncations up to  $\mathcal{O}(\mu_B^{10})$ .

phase of QCD, the medium is composed of hadrons and their resonances. In its simplest version, the hadron resonance gas (HRG) model assumes that the constituents of the medium are independent and point-like [18]. This effectively neglects their widths and interactions. Consequently, the pressure in the HRG model is approximated by the sum over partial pressures of hadrons and their resonances, treated as noninteracting particles,

$$P = \sum_i P_i, \quad (10)$$

where  $i$  goes through all strange and non-strange hadrons and their resonances listed in the Particle Data Group summary tables [19]<sup>#1</sup>. We note that the thermodynamic pressure  $P$  contains all the relevant information about the medium through the mass and the quantum numbers of hadrons. Thus, it allows for the study of different thermodynamic observables, including particle numbers and fluctuations of conserved charges.

The partial pressures in Eq. (10) are given as

$$P_i = \mp \gamma_i T \int \frac{d^3p}{(2\pi)^3} \ln(1 \mp f_i), \quad (11)$$

where  $T$  is temperature,  $\gamma_i$  is the spin degeneracy factor, and

$$f_i = \left( e^{(\epsilon_i - \mu_i)/T} \pm 1 \right)^{-1} \quad (12)$$

<sup>#1</sup> In this work, we include established mesons and baryons with three- and four-star rating.

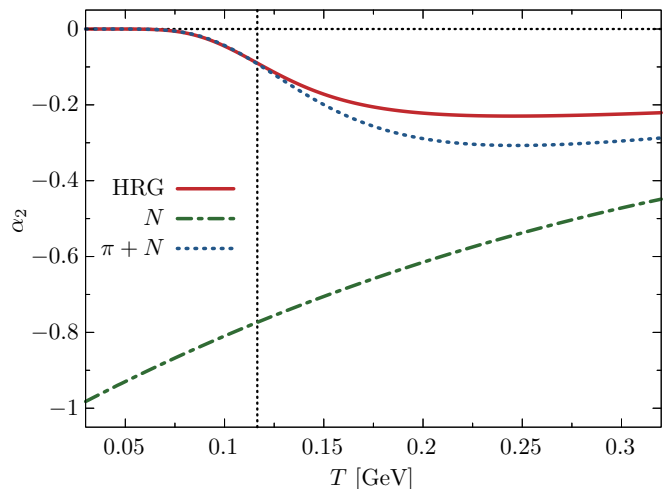


FIG. 4. The coefficient  $\alpha_2$  for the HRG model, as well as a gas of nucleons and a gas of pions and nucleons. The vertical, dotted line marks the temperature at which the second derivative vanishes, i.e.,  $\alpha_2'' = 0$  in the full HRG model.

is the distribution function,  $\epsilon_i = \sqrt{p^2 + m_i^2}$  is the dispersion relation and  $\mu_i = B_i\mu_B + Q_i\mu_Q + S_i\mu_S$  is the chemical potential of the particle. In this work, we set  $\mu_Q = \mu_S = 0$ . The upper (lower) signs in Eqs. (11) and (12) refer to fermions (bosons).

We use the HRG model to calculate the Taylor expansion coefficients  $\alpha_k$ , defined in Eq. (3). In Fig. 1, we show the non-vanishing coefficients up to  $k = 10$  at  $\mu_B = 0$ . Higher-order coefficients become more complex. For convenience, we denote the expansion truncated at order  $k$  by superscript  $(k)$ . We are primarily interested in the expansion of the HRG model truncated at  $k = 2$ .

To locate the putative CP, one needs to solve Eqs. (8). The first and second temperature derivatives of  $\alpha_2$  are shown in Fig. 2. We find that  $d^2\alpha_2/dT^2 = 0$  at  $T_0^c = 0.117$  GeV. This yields  $(T_c^{(2)}, \mu_{B,c}^{(2)}) = (0.086, 0.823)$  GeV for the location of the CP. We stress that the HRG model does not predict any CP, because there is no criticality built-in in this model. Therefore, the second-order expansion leads to a nonphysical approximation of the full HRG model. This is shown in Fig. 3, where we show the constant-entropy contour that leads to the fake CP. This is in contrast with the full HRG contour, which deviates from the truncated one as the baryon chemical potential increases. At  $\mu_{B,c}^{(2)} = 0.823$  GeV, the truncated contour lies at a temperature higher than the one obtained in the full HRG by 60%.

We also considered the expansion truncated at the fourth order of the expansion, i.e.,  $k = 4$ . This model leads to  $(T_c^{(4)}, \mu_{B,c}^{(4)}) = (0.066, 0.843)$  GeV. Thus, even the fourth-order expansion leads to a nonphysical prediction of the location of the CP.

To better understand why the second-order expansion leads to an unphysical CP, we consider a single-

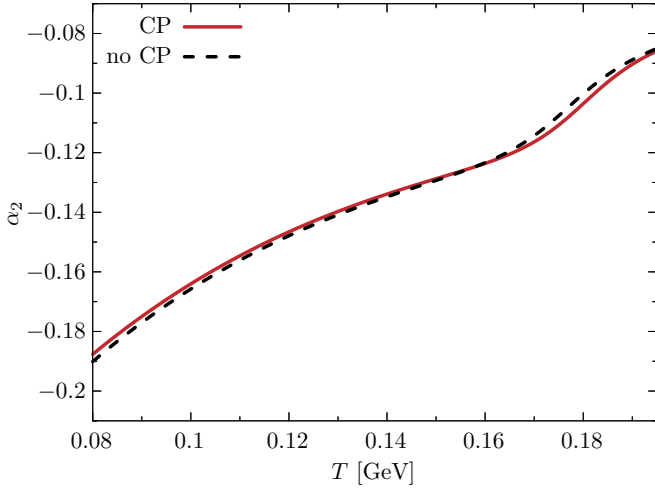


FIG. 5. The expansion parameters  $\alpha_2$  in two different schemes, one with (solid red line) and one without a CP (dashed black line).

component ideal gas. In this case, one may show that

$$\alpha_2 \xrightarrow{T \rightarrow 0} -\frac{B^2}{M}, \quad (13)$$

where  $M$  is the particle's mass and  $B$  is its baryon number. Thus,  $\alpha_2 \rightarrow 0$  for mesons and  $\alpha_2 \rightarrow -M^{-1}$  for baryons as the temperature approaches zero. The limit in Eq. (13) can be straightforwardly generalized to a multi-component gas of ideal particles, in which case the limit is determined by the lightest hadron.

The behavior of  $\alpha_2$  in the system of nucleons is shown in Fig. 4. It is an increasing function of temperature. Therefore, the solution of Eqs. (8) does not lead to any prediction of CP at finite baryon chemical potential. On the other hand, for a system of pions and nucleons,  $\alpha_2$  starts from zero, decreases, and develops a minimum at  $T > 0.2$  GeV. Consequently, it features an inflection point, and the solution of Eqs. (8) leads to a prediction of CP at  $(T_c^{(\pi N)}, \mu_{B,c}^{(\pi N)}) = (0.086, 0.816)$  GeV. We note that the values are very close to those obtained in the truncated HRG model with the full resonance spectrum. This is so because at  $T \lesssim 0.12$  GeV the thermodynamic pressure is predominantly due to pions and nucleons. This reassures that the inflection point of  $\alpha_2$  that leads to the prediction of an unphysical CP in the full HRG model is obtained primarily due to the presence of pions and nucleons in the particle spectrum and should not depend on the list of resonances used in the calculations. We have verified this for the list of resonances that includes the prediction from the quark model [20, 21].

#### IV. NAMBU–JONA-LASINIO MODEL

The NJL model Lagrangian for two quark flavors with a degenerate quark mass  $m_0$  and the isoscalar vector in-

set	$G_S \Lambda^2$	$\Lambda$ [MeV]	$m_0$ [MeV]	source
1	2.083	665.0	5.0	[22]
2	2.060	664.3	5.0	[8]
3	4.3479	364.69	5.0	this work

TABLE I. Parameters of the NJL model used in this work.

teraction reads [8]

$$\mathcal{L}_{\text{NJL}} = \bar{\psi}(i\gamma^\mu \partial_\mu - m_0)\psi + G_S[(\bar{\psi}\psi)^2 + (\bar{\psi}i\gamma_5\vec{\tau}\psi)^2] - G_V(\bar{\psi}\gamma_\mu\psi)^2. \quad (14)$$

In the mean-field approximation, the effective thermodynamic potential is given by [8]

$$\Omega_{\text{NJL}} = \frac{(M - m_0)^2}{4G_S} - \frac{(\mu - \tilde{\mu})^2}{4G_V} + \Omega_{\text{vac}} + \Omega_{\text{th}}, \quad (15)$$

where

$$\Omega_{\text{vac}} = -12 \int_{|\mathbf{p}| < \Lambda} \frac{d^3p}{(2\pi)^3} \epsilon_q \quad (16)$$

with  $\epsilon_q = \sqrt{\mathbf{p}^2 + M^2}$  is the vacuum contribution which we regularize with the sharp three-momentum cutoff. The thermal contribution reads

$$\Omega_{\text{th}} = 12T \int \frac{d^3p}{(2\pi)^3} (\ln(1 - f) + \ln(1 - \bar{f})) \quad (17)$$

and does not require regularization since the integral is convergent. The Fermi-Dirac distributions for quark and antiquarks read

$$f = \left( e^{(\epsilon_q - \tilde{\mu})/T} + 1 \right)^{-1}, \quad \bar{f} = \left( e^{(\epsilon_q + \tilde{\mu})/T} + 1 \right)^{-1} \quad (18)$$

respectively. The gap equations can be obtained from the effective potential [8],

$$\frac{\partial \Omega_{\text{NJL}}}{\partial M} = 0, \quad \frac{\partial \Omega_{\text{NJL}}}{\partial \tilde{\mu}} = 0. \quad (19)$$

In general, the phase diagram obtained in the NJL model, and thus the existence and location of the critical point is regularization scheme dependent [22]. In this work, we use two different schemes, for which the parameters can be seen in Tab. I. The first scenario yields a CP at  $\mu_B \approx 990$  MeV and  $T \approx 19$  MeV (Set 1), while the second does not predict the existence of a CP (Set 2).

In Fig. 5, we show the expansion parameter  $\alpha_2$  obtained in these two models. Both parameters increase with temperature and exhibit very similar behavior, even though only one of the models predicts the CP. Consequently, from the lowest-order expansion, there is no sign of criticality from the CP, although one of the models (Set 1) features a CP in the phase diagram.

Another well-known feature of the NJL model is that the increase of the vector coupling moves the critical

$\hat{G}_V$	$T_0^c$ [GeV]	$\alpha_2'(T_0^c)$ [GeV $^{-2}$ ]	$\alpha_2(T_0^c)$ [GeV $^{-1}$ ]	$\mu_B^{\text{pred.}}$ [GeV]	$T_c^{\text{pred.}}$ [GeV]	$\mu_B^{\text{NJL}}$ [GeV]	$T_c^{\text{NJL}}$ [GeV]
0.000	0.16097	-74.398	-0.1925	0.164	0.158	0.100	0.160
0.075	0.16096	-12.41	-0.1316	0.401	0.150	0.330	0.153
0.100	0.16094	-5.279	-0.1182	0.616	0.139	0.477	0.146
0.125	0.16090	-1.883	-0.1066	1.031	0.104	0.618	0.137
0.167	0.16040	0	-0.091	—	—	0.789	0.124
0.250	—	—	—	—	—	1.008	0.104

TABLE II. Results obtained by applying the constant-entropy expansion to the NJL model (parameter set 3) for different values of the dimensionless repulsive coupling  $\hat{G}_V$ . Predicted critical baryon chemical potential and temperature are compared with the results obtained directly from the model.

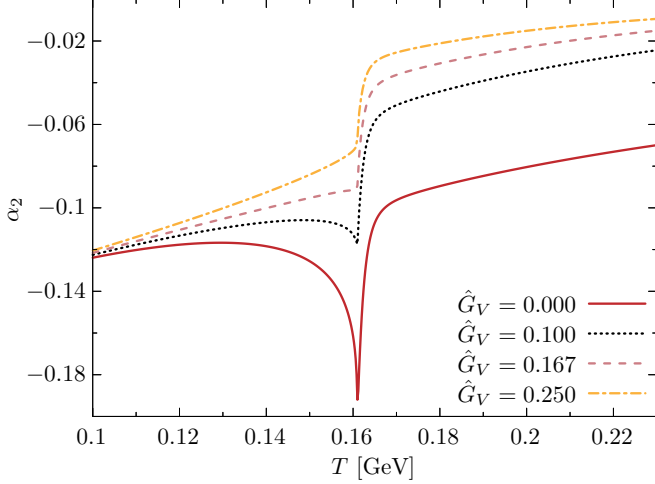


FIG. 6. The expansion parameter  $\alpha_2$  in the NJL model for different values of the dimensionless vector coupling  $\hat{G}_V$ .

point towards lower temperatures until it vanishes for the critical value of the coupling [8, 23]. We use these features of the model to adjust the location of the critical point and study the predictive power of the expansion (2). If the critical point lies close to  $\mu_B = 0$ , where the expansion was performed, its effect is expected to appear even in the lower order coefficients. However, as the CP moves to larger chemical potentials, its effect on the  $\mu_B = 0$  thermodynamics is reduced, and one needs higher (if not infinite) orders in the expansion to be sensitive to the criticality [24]. This explains, why parameter sets 1 and 2 of the NJL model lead to almost the same  $\alpha_2$ .

To further study the expansion truncated at the second order, we consider an artificial parameterization (see the bottom row of Tab. I) of the NJL model chosen such that the critical point is located at exceptionally low  $\mu_B \approx 100$  MeV and high  $T \approx 160$  MeV for vanishing vector coupling  $G_V = 0$ . We stress that such parametrization is not expected to match the known phenomenology, e.g., the pion mass or the quark condensate, but serves merely as a tool to study the expansion under consideration. By increasing  $\hat{G}_V \equiv G_V/G_S$  for a fixed value of  $G_S$ , the CP shifts towards smaller temperatures and higher chemical potentials and vanishes for the critical value of

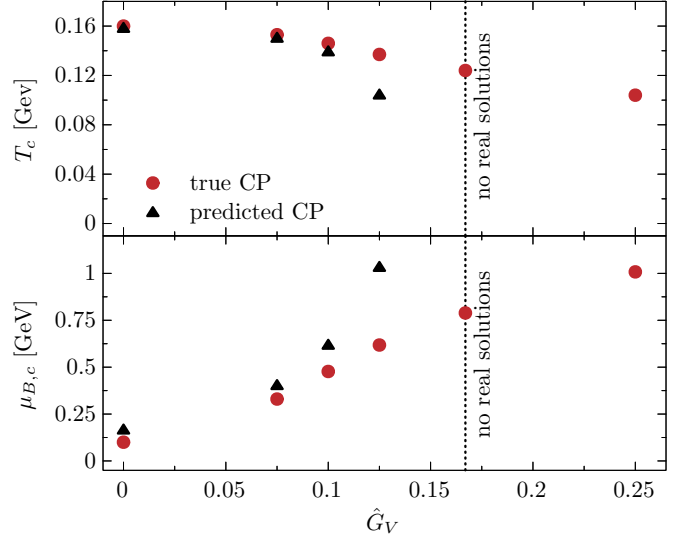


FIG. 7. The location of the true (circles) and predicted (triangles) critical points in terms of temperature (top) and baryon chemical potential (bottom) as a function of the dimensionless repulsive coupling  $\hat{G}_V$  in the NJL model. The vertical dotted line marks  $\hat{G}_V$  above which there is no prediction for the CP in the truncated NJL model (see text for details).

the coupling  $\hat{G}_V = 0.94$ .

The  $\alpha_2$  curves for several values of  $\hat{G}_V$  are shown in Fig. 6. We observe strong sensitivity to the value of the vector coupling. Particularly, the dip seen in the vicinity of the pseudo-critical temperature becomes shallower as  $\hat{G}_V$  increases and vanishes for  $\hat{G}_V = 0.167$ .

By utilizing Eqs. (8), we obtained predictions for the CP for different values of  $\hat{G}_V$ . Our findings are summarized in Tab. II. We observe that predictions for the location of the CP become worse as  $\hat{G}_V$  increases, i.e. CP becomes more distant from the  $\mu_B = 0$  line. For  $\hat{G}_V = 0$  the prediction for  $\mu_B$  differs by  $\approx 60$  MeV, while for  $\hat{G}_V = 0.125$  the difference exceeds 400 MeV. The predictions for  $T_c$  are more accurate but also worsen with the increasing vector coupling. Particularly, for  $\hat{G}_V = 0.167$  and larger, the method fails to predict the existence of the CP. This behavior can be understood as follows: for small values of  $\hat{G}_V$ , there is an inflection point in  $\alpha_2$

with  $d\alpha_2/dT < 0$ , which gives a prediction for the CP at finite and positive  $\mu_B$ . As  $\hat{G}_V$  increases, the dip becomes shallower and disappears, hence  $d\alpha_2/dT \rightarrow 0^-$ , and the predicted value of the baryon chemical potential approaches  $\infty$ , while the predicted value of  $T \rightarrow -\infty$ . In the present setup, this happens for  $\hat{G}_V = 0.167$ .

For larger values of the vector coupling, we observe that  $\alpha_2$  is monotonically increasing in temperature, and there is no prediction for a real baryon chemical potential, even though there is a CP in the full model. In Fig. 7 we compare the actual and predicted values of  $T$  (upper panel) and  $\mu_B$  (lower panel) for different values of  $\hat{G}_V$ . The dashed line marks the value of the coupling above which Eqs. (8) have no real solutions.

If the CP is sufficiently far, the expansion cannot account for its effect in the lowest order. This highlights the limited validity of this approximation. We emphasize that our artificial parametrization demonstrates the limitation of the truncated expansion qualitatively, however, it does not provide a quantitative prediction for the range of its usability.

We note that, due to the absence of the dynamical mesons in the NJL model,  $\alpha_2$  behaves similarly to the HRG result with only the baryons present, tending to a negative value for  $T \rightarrow 0$ . On the other hand, if the Polyakov loop is included for the effective confinement, one has  $\alpha_2 \rightarrow 0$  as the temperature vanishes. Therefore, there is an additional inflection point, which always gives a prediction for the CP, even if the model has no criticality. However, this inflection point and the predicted CP have no connection to the chiral transition.

Finally, one can also include meson fluctuations in the quark-meson (QM) model – which gives qualitatively the same results as the NJL model – in an ideal-gas or Gaussian approximation [25]. Similarly to the Polyakov loop, the dynamical mesons lead to  $\alpha_2 \rightarrow 0$  for  $T \rightarrow 0$  in agreement with the HRG results. Consequently, the expansion in such an extended QM model predicts the existence of a CP for any parametrization of the model, although it is not related to the chiral phase transition.

## V. CONCLUSION

We have considered the constant-entropy-density-contour expansion scheme, which was recently proposed

for the search of the putative critical point in the QCD phase diagram [13]. We have applied the scheme to the hadron resonance gas model, which does not predict the existence of any CP because of the lack of criticality built into it. Nevertheless, we find that the expansion scheme truncated at the second-order Taylor coefficient yields a prediction for the CP at finite temperature and baryon chemical potential. By analyzing the expansion coefficient, we found that the prediction of the CP is due to the presence of both mesonic and baryonic degrees of freedom, and thus is not necessarily a signal of a CP.

We have also considered the Nambu–Jona-Lasinio model which captures the spontaneous breaking of the chiral symmetry and its restoration and thus may predict the existence of CP, depending on the parameterization. Utilizing different regularization schemes, we demonstrated that the expansion at the lowest truncation order is not sensitive to the critical effects unless the critical point is located exceptionally close to the  $\mu_B = 0$  line. We also found that the method under consideration may fail to predict the existence of the CP, even though it is present in the full model. This spotlights its limited applicability and suggests that further careful analysis of the expansion scheme is required.

## ACKNOWLEDGMENTS

The authors are thankful for the valuable discussion with P. M. Lo, K. Redlich, and C. Sasaki. M. M. acknowledges the support through the program Excellence Initiative–Research University of the University of Wrocław of the Ministry of Education and Science. M. S. acknowledges the financial support of the Polish National Science Center (NCN) under the Preludium grant 2020/37/N/ST2/00367. The work of G. K. is partially supported by the Polish National Science Centre (NCN) under OPUS Grant No. 2022/45/B/ST2/01527.

- 
- [1] A. Bazavov *et al.* (HotQCD), Equation of state in (2+1)-flavor QCD, Phys. Rev. **D90**, 094503 (2014), arXiv:1407.6387 [hep-lat].
  - [2] S. Borsanyi, Z. Fodor, J. N. Guenther, S. K. Katz, K. K. Szabo, A. Pasztor, I. Portillo, and C. Ratti, Higher order fluctuations and correlations of conserved charges from lattice QCD, JHEP **10**, 205, arXiv:1805.04445 [hep-lat].
  - [3] A. Bazavov *et al.*, The QCD Equation of State to  $\mathcal{O}(\mu_B^6)$  from Lattice QCD, Phys. Rev. D **95**, 054504 (2017), arXiv:1701.04325 [hep-lat].
  - [4] A. Bazavov *et al.*, Skewness, kurtosis, and the fifth and sixth order cumulants of net baryon-number distributions from lattice QCD confront high-statistics STAR data, Phys. Rev. D **101**, 074502 (2020), arXiv:2001.08530 [hep-lat].
  - [5] Y. Aoki, G. Endrodi, Z. Fodor, S. Katz, and K. Szabo, The Order of the quantum chromodynamics transition predicted by the standard model of particle physics, Na-

- ture **443**, 675 (2006), arXiv:hep-lat/0611014.
- [6] E. S. Bowman and J. I. Kapusta, Critical Points in the Linear Sigma Model with Quarks, *Phys. Rev. C* **79**, 015202 (2009), arXiv:0810.0042 [nucl-th].
  - [7] L. Ferroni, V. Koch, and M. B. Pinto, Multiple Critical Points in Effective Quark Models, *Phys. Rev. C* **82**, 055205 (2010), arXiv:1007.4721 [nucl-th].
  - [8] M. Buballa, NJL model analysis of quark matter at large density, *Phys. Rept.* **407**, 205 (2005), arXiv:hep-ph/0402234.
  - [9] C. Sasaki, B. Friman, and K. Redlich, Chiral phase transition in the presence of spinodal decomposition, *Phys. Rev. D* **77**, 034024 (2008), arXiv:0712.2761 [hep-ph].
  - [10] M. M. Aggarwal *et al.* (STAR), An Experimental Exploration of the QCD Phase Diagram: The Search for the Critical Point and the Onset of De-confinement (2010), arXiv:1007.2613 [nucl-ex].
  - [11] M. Maćkowiak-Pawłowska (NA61/SHINE), NA61/SHINE results on fluctuations and correlations at CERN SPS energies, *Nucl. Phys. A* **1005**, 121753 (2021), arXiv:2002.04847 [nucl-ex].
  - [12] A. Bzdak, S. Esumi, V. Koch, J. Liao, M. Stephanov, and N. Xu, Mapping the Phases of Quantum Chromodynamics with Beam Energy Scan, *Phys. Rept.* **853**, 1 (2020), arXiv:1906.00936 [nucl-th].
  - [13] H. Shah, M. Hippert, J. Noronha, C. Ratti, and V. Vovchenko, Locating the QCD critical point from first principles through contours of constant entropy density (2024), arXiv:2410.16206 [hep-ph].
  - [14] S. Borsanyi, Z. Fodor, J. N. Guenther, P. Parotto, A. Pasztor, C. Ratti, V. Vovchenko, and C. H. Wong, Lattice QCD constraints on the critical point from an improved precision equation of state (2025), arXiv:2502.10267 [hep-lat].
  - [15] A. Bazavov *et al.* (HotQCD), Equation of state in (2+1)-flavor QCD, *Phys. Rev. D* **90**, 094503 (2014), arXiv:1407.6387 [hep-lat].
  - [16] D. Bollweg, J. Goswami, O. Kaczmarek, F. Karsch, S. Mukherjee, P. Petreczky, C. Schmidt, and P. Scior (HotQCD), Second order cumulants of conserved charge fluctuations revisited: Vanishing chemical potentials, *Phys. Rev. D* **104**, 10.1103/PhysRevD.104.074512 (2021), arXiv:2107.10011 [hep-lat].
  - [17] A. Andronic, P. Braun-Munzinger, K. Redlich, and J. Stachel, Decoding the phase structure of QCD via particle production at high energy, *Nature* **561**, 321 (2018), arXiv:1710.09425 [nucl-th].
  - [18] P. Braun-Munzinger, K. Redlich, and J. Stachel, Particle production in heavy ion collisions (2003), arXiv:nucl-th/0304013.
  - [19] R. L. Workman *et al.* (Particle Data Group), Review of Particle Physics, *PTEP* **2022**, 083C01 (2022).
  - [20] U. Loring, B. C. Metsch, and H. R. Petry, The Light baryon spectrum in a relativistic quark model with instanton induced quark forces: The Strange baryon spectrum, *Eur. Phys. J. A* **10**, 447 (2001), arXiv:hep-ph/0103290.
  - [21] D. Ebert, R. N. Faustov, and V. O. Galkin, Mass spectra and Regge trajectories of light mesons in the relativistic quark model, *Phys. Rev. D* **79**, 114029 (2009), arXiv:0903.5183 [hep-ph].
  - [22] H. Kohyama, D. Kimura, and T. Inagaki, Regularization dependence on phase diagram in Nambu–Jona-Lasinio model, *Nucl. Phys. B* **896**, 682 (2015), arXiv:1501.00449 [hep-ph].
  - [23] C. Sasaki, B. Friman, and K. Redlich, Quark Number Fluctuations in a Chiral Model at Finite Baryon Chemical Potential, *Phys. Rev. D* **75**, 054026 (2007), arXiv:hep-ph/0611143 [hep-ph].
  - [24] F. Karsch, B.-J. Schaefer, M. Wagner, and J. Wambach, Towards finite density QCD with Taylor expansions, *Phys. Lett. B* **698**, 256 (2011), arXiv:1009.5211 [hep-ph].
  - [25] G. Kovács, P. Kovács, and Z. Szép, One-loop constituent quark contributions to the vector and axial-vector meson curvature mass, *Phys. Rev. D* **104**, 056013 (2021), arXiv:2105.12689 [hep-ph].